ARRAYS OF SOLVENT CAST HOLLOW OUT-OF-PLANE MICRONEEDLES FOR DRUG DELIVERY

I. Mansoor, U.O. Häfeli, and B. Stoeber
The University of British Columbia, Vancouver, British Columbia, CANADA

ABSTRACT

Microneedles are tiny hollow structures that allow painless drug delivery into human skin. In this work, we present a novel method based on solvent casting for rapid fabrication of inexpensive microneedles from polymer materials. The polymer microneedles are formed on a reusable mold made with a single photolithography step. The strength of the fabricated microneedles under compressive loading was investigated. The capability of the microneedles for drug delivery was also demonstrated by injection of fluorescent beads into rabbit ear skin and inspection of the penetration depth using confocal microscopy.

INTRODUCTION

In recent years, substantial research has been carried out to find new drug delivery ways to replace traditional methods such as oral administration, skin patches, and injection using hypodermic needles. One promising novel method is using microneedles for transdermal drug injection. Microneedles are solid or hollow pointed sub-millimeter devices that can pierce skin and deliver a compound [1]. In contrast to adhesive skin patches which rely on drug absorption from the skin surface, microneedles penetrate through the stratum corneum (the outermost layer of the skin with a thickness of up to 20 µm [2]) and deliver the drug directly underneath it; as a result, microneedles increase skin permeability to several hydrophilic and lipophilic compounds, and therefore can potentially allow administration of a much wider range of drugs compared with adhesive patches. They also do not penetrate deeper than the skin's epidermis layer (with a typical thickness of 100 µm [2]) to contact nerves and blood vessels and therefore, they are painless [3] and less associated with the risks of device contamination. In previous works, several prototypes for solid and hollow out-of-plane microneedles have been presented. These devices have mainly been fabricated out of silicon [4], polysilicon [5], metals [6], glass [7], and polymers [8]. In most cases, the fabrication processes for making hollow devices are expensive and/or require multiple molding and photolithography steps.

While the commercial adoption of microneedle has mainly been impeded by the previously proposed long and expensive fabrication processes, solvent casting offers a rapid and inexpensive alternative to those methods. For more than a century, solvent casting has been a common method for forming polymer films [9]. In this method, a polymer solution is applied to a mold and after evaporation of the solvent a film is formed that is then separated from the mold by chemical or physical means. Solvent casting can also be used to fabricate MEMS devices from polymer materials and can provide a cheaper alternative to current expensive processes. Previous works have used this method to coat microchannels with a variety of polymers such as poly(vinyl alcohol), poly(ethylene oxide), poly(*N*-hydroxyethylacrylamide), and polyacrylamide; the applications were protein and DNA separation as well as the modification of surface properties [10]. Additionally, solvent casting has been used to create structural layers on top of sacrificial layers that are later dissolved. Polyactic acid microstructures for tissue engineering have been previously fabricated using this technique [11]. It is previously shown that by controlling some process parameters in the solvent casting process, such as temperature, the final shape and thickness of the polymer profile in the mold can be controlled [12]. Controlling such parameters, therefore, can be crucial when fabricating MEMS devices with this method.

In this work, we demonstrate a new solvent casting method for rapid fabrication of hollow out-of-plane polymer microneedles requiring only one step of photolithography. Our process uses a single mold for consecutive solvent casting of polymer films, eliminating the need of mask alignment. The needles were tested for mechanical robustness, and injection of fluorescent beads into rabbit ear skin was demonstrated.

FABRICATION

Our solvent casting process uses SU-8 for the mold and 2% nanoclay-reinforced polyimide as the structural material for the needles due to its high Young's modulus [13]. The fabrication process for the microneedles is illustrated in Figure 1. Using photolithography, an array of 450 µm-high cylindrical pillars is fabricated from SU-8 2150 (Microchem, US) on a 300 µm thick Pyrex glass substrate (Figure 1a, b). The UV exposure of the SU-8 is performed through the glass substrate in order to take advantage of the effect of UV light diffraction caused by the gap between the photomask and the photoresist [14]. This technique results in tapered pillars with the wider end attached to the glass substrate. These pillars form the mold structure and will define the needle lumens. Polydimethylsiloxane (PDMS) SYLGARD 184 (Dow Corning, US) is then spun onto the mold structure and cured in an oven at 65ºC. The resulting 30-µm PDMS layer improves the rigidity of the mold structure and also exhibits a poor adhesion with polyimide, and therefore facilitates easy removal of the microneedle array from the mold (Figure 1c, Figure 2). After PDMS deposition, the mold is ready and can be used for consecutive fabrication of microneedles. The fabrication of the mold takes approximately 5 hr.

Polyimide solvent (*N*-Methyl-2-pyrrolidone, NMP) is

added to the polyimide/nanoclay mixture at a weight ration of 2:1.5. After an O_2 plasma treatment of the mold, this solution is deposited onto the pillars (Fig. 1d, e). The plasma treatment temporarily improves surface wetting of the PDMS by the polyimide solution and therefore leads to coverage of the entire pillars, resulting in taller and sharper structures.

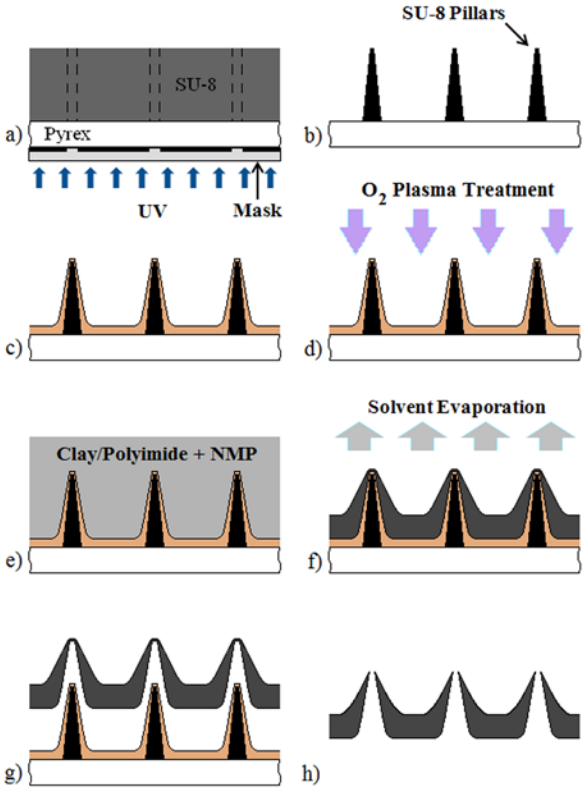

Figure 1: Fabrication process using solvent casting for hollow out-of-plane polymer microneedles a & b) fabrication of pillars from SU-8 c) PDMS deposition d) O_2 plasma treatment of the mold e) clay/polyimide + NMP deposition f) Evaporation of NMP g) removing of the microneedle array from the mold h) opening of the microneedle tips.

After solvent evaporation in a soft baking process at 100ºC, the polymer will automatically form the microneedle arrays including thin walls around the pillars and wide bases as well as a thick backing plate (Figure 1f). The polyimide layer is then separated from the mold by mechanical force (Figure 1g) and is then cured in a nitrogen atmosphere at 300ºC. The needle tips are then opened by either O_2/CF_4 plasma etching, or by using fine 3 µm aluminum oxide sanding paper (Figure 1h).

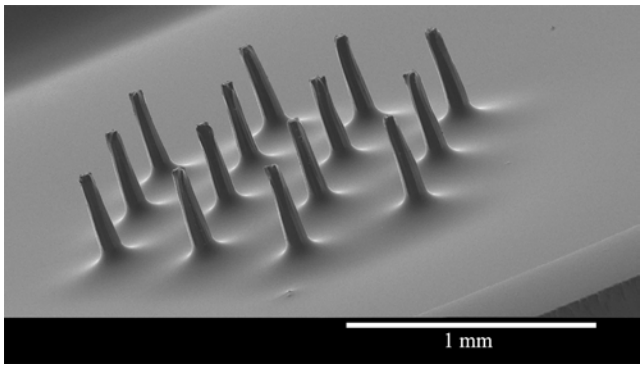

Figure 2: SEM of a mold consisting of pillars from SU-8 and a coating of PDMS; the distance between the pillars in the array is 500 µm.

The resulting microneedles are 250 µm high with an average tip diameter of 50 µm (Figure 3a, b, c). The entire solvent casting process, including the curing of the microneedles as well as opening their tips, takes about 6 hr.

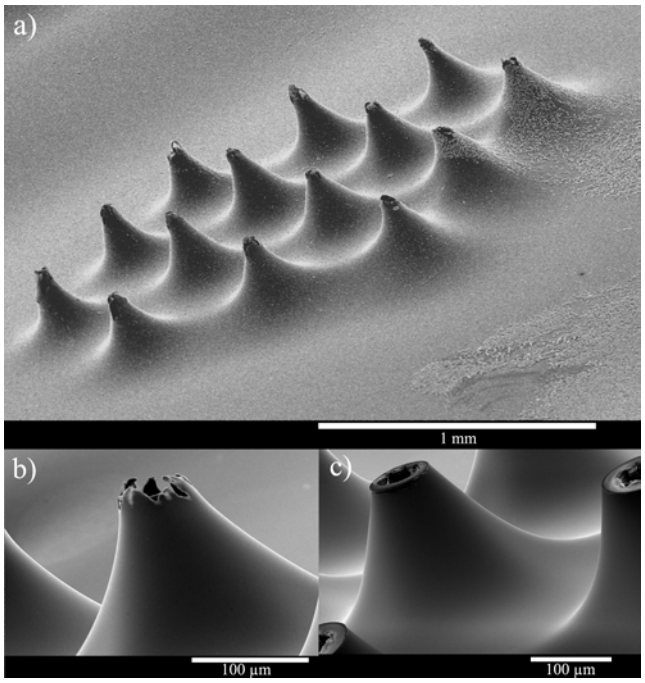

Figure 3: SEM image of a microneedle array. a) an array of 14 needles opened by plasma etching, b) a needle opened by plasma etching and c) a needle opened by sanding.

TESTING THE MICRONEEDLES

Mechanical Tests

In order to investigate the strength of the fabricated microneedles, a Physica MCR rheometer (Anton Paar) was used to apply vertical compressive loads to individual needles. For this purpose, molds containing single pillars were made using a different photolithography mask, and the same microneedle fabrication process was used to make the individual needles from those molds. The mechanical tests

were performed on ten needles and the corresponding force vs. displacement graphs were obtained for analysis.

Figure 4a shows an example of a force vs. displacement plot. The sudden drop of the force in the plot corresponds to the needle tip failing and therefore indicates the failure load. Figure 4b shows a failed needle after loading; in this figure, the upper portion of the device is ruptured and bent almost at the midpoint of its height, while the lower portion is still rigid. From the data for the ten needles tested, it was observed that on average each needle can sustain an in-plane compressive load of 0.32 ± 0.06 N.

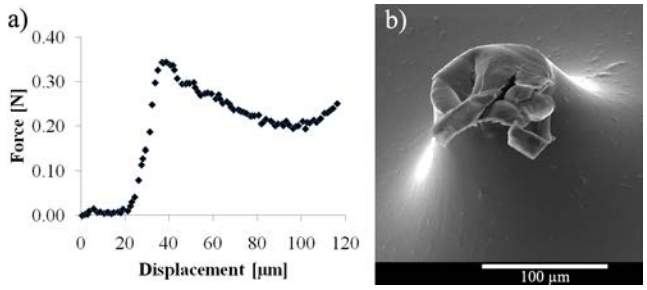

Fig. 4: a) Example of a needle tip displacement under axial loading; b) SEM of a failed needle

A previous study has investigated the force required for insertion of various designs of microneedles into human skin [15]. According to this study, the insertion force mainly depends on the interfacial area, defined as the total microneedle tip area. The experimental data from insertion of various designs of microneedles, with a wide range of tip diameters, into human skin suggest that the fabricated devices in this work penetrate the skin without failure.

Injection Tests

In order to demonstrate the capability of the fabricated devices for epidermal drug delivery, a series of injection tests were carried out. For this purpose, a 0.025 wt% solution of 0.21 µm polystyrene fluorescent beads in water was prepared and injected into the inner skin of a rabbit ear. The injection was performed using the fabricated microneedles which were bonded to the flat end of a conventional 1 ml syringe. During the injection, the needles were pressed against the skin for about 10 s with a moderate force. Rabbit skin was chosen for this study due to its potential as a human skin model for in vitro transdermal permeation studies [16]. Traditionally, pig skin has been considered as the best model to replace human skin for in vitro tests due to their biochemical similarly [17, 18]. However, the main drawback of using other animal skins including the pig skin is that the permeability of these skins is much higher than that of human especially to hydrophilic agents. Having a considerably less permeability to hydrophilic compounds compared with traditional skin models, rabbit ear skin is proved to be a reasonable model for human skin [16].

A total of six injection trials using the fabricated microneedles were carried out and after each trial, the injection site on the skin was imaged using a D-Eclipse C1 confocal microscope (Nikon). The skin was scanned down to a depth of 200 µm to observe the penetration depth of the fluorescent beads. Figure 5a shows the fluorescent beads at different depths under the skin after an injection trial.

After each scan, the penetration depth of the fluorescent beads under the skin was analyzed from the intensity distribution of the detected fluorescence from the confocal slices. For this purpose, MATLAB was used to obtain the total intensity in each slice, and the average penetration depth and its 95% distribution interval was obtained from the corresponding histogram distribution.

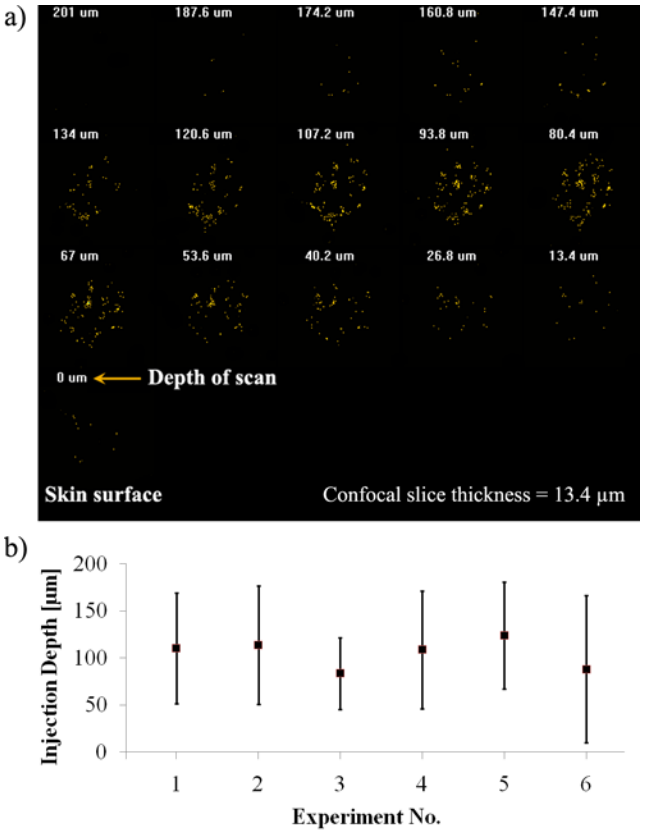

Fig. 5: a) Tiled arrangement of the confocal images of an injection site, b) average depth (squares) and range (bars) of the injected fluorescence from six trials, obtained from the intensity distribution and its 95% distribution interval; the average injection depth for all trials was 104.8 ± 15.6 µm and the average of all ranges of distribution was 119 ± 25.8 µm

Results from the six injection trials showed average delivery depths for the fluorescent beads of 104.8 ± 15.6 µm over an average depth range of 119 ± 25.8 µm, indicating successful delivery into the epidermis, past the stratum corneum (Figure 5b).

CONCLUSIONS

A new process, based on solvent casting, has been presented for the fabrication of hollow out-of-plane microneedles from polymers. The proposed process is relatively fast and inexpensive, and is therefore applicable for mass production of cheap microneedle devices. By changing the dimensions of the pillars in the mold, microneedles with different lengths and lumen diameters can be fabricated. Additionally, other polymers can be used in the same process to make microneedles after adjusting the process conditions.

The strength of the fabricated devices was tested by applying vertical compressive loads to individual needles. It was found that the needles are strong enough to puncture human skin without failure. Additionally, epidermal delivery using the fabricated needles was tested by injection of a suspension of fluorescent beads into rabbit ear skin. The confocal images of the injection sites revealed successful penetration of the beads in the skin.

ACKNOWLEDGEMENTS

The authors would like to acknowledge financial support provided by CMC Microsystems (www.cmc.ca) that partly funded the fabrications costs of this research through the MNT Financial Assistance program. The authors also acknowledge financial support from the Natural Sciences and Engineering Research Council of Canada (NSERC) though the Collaborative Health Research Projects program, as well as the British Columbia Innovation Council through the BCIC Innovation Scholarship award.

REFERENCES

[1] M. R. Prausnitz, "Microneedles for Transdermal Drug Delivery", *Adv. Drug Deliver. Rev.*, vol. 56, pp. 581-587, 2004.

[2] H. Schaefer, T. E. Redelmeier, *Skin Barrier*. Basel, Switzerland: Karger, 1996.

[3] R. K. Sivamani, B. Stoeber, G. C. Wu, H. Zhai, D. Liepmann, H. Maibach, "Clinical Microneedle Injection of Methyl Nicotinate: Stratum Corneum Penetration", *Skin Res. Technol.*, vol. 11, pp. 152-156, 2005.

[4] B. Stoeber, D. Liepmann, "Arrays of Hollow Out-of-Plane Microneedles for Drug Delivery", *J. Microelectromech. Syst.*, vol. 14, pp. 472-479, 2005.

[5] J. D. Zahn, N. H. Talbot, D. Liepmann, A. P. Pisano, "Microfabricated Polysilicon Microneedles for Minimally Invasive Biomedical Devices", *Biomed. Microdevices*, vol. 2, pp. 295-303, 2000.

[6] S. P. Davis, W. Martanto, M. G. Allen, M. R. Prausnitz, "Hollow Metal Microneedles for Insulin Delivery to Diabetic Rats", in *IEEE T. Biomed. Eng.*, vol. 52, pp. 909-915, 2005.

[7] P. M. Wang, M. Cornwell, J. Hill, M. R. Prausnitz, "Precise Microinjection into Skin Using Hollow Microneedles", *J. Invest. Dermatol.*, vol. 126, pp. 1080-1087, 2006.

[8] J. H. Park, M. G. Allen, M. R. Prausnitz, "Biodegradable Polymer Microneedles: Fabrication, Mechanics and Transdermal Drug Delivery", *J. Control. Release*, vol. 104, pp. 51-66, 2005.

[9] U. Siemann, "Solvent Cast Technology–A Versatile Tool for Thin Film Production", *Prog. Coll. Pol. Sci.*, vol. 130, pp 1-14, 2005.

[10] E. A. S. Doherty, R. J. Meagher, M. N. Albarghouthi, A. E. Barron, "Microchannel wall coatings for protein separations by capillary and chip electrophoresis", *Electrophoresis*, vol. 24, pp. 34-54, 2003.

[11] G. J. Wang, K. H. Ho, C. C. Hsueh, "Biodegradable polyactic acid microstructures for scaffold applications", *Microsyst. Technol.*, vol. 14(7), pp. 989-993, 2008.

[12] I. Mansoor, B. Stoeber, "PIV Measurements of Flow in Drying Polymer Solutions during Solvent Casting", *Exp. Fluids*, In press, 2010.

[13] T. Agag, T. Koga, T. Takeichi, "Studies on Thermal and Mechanical Properties of Polyimide-clay Nanocomposites", *Polymer*, vol. 42(8): pp. 3399-3408, 2001.

[14] M. C. Peterman, P. Hulie, D. M. Bloom, H. A. Fishman, "Building Thick Photoresist Structures From the Bottom Up", *J. Micromech. Microeng.*, vol. 13(3), pp. 380-382, 2003.

[15] S. P. Davis, B. J. Landis, Z. H. Adams, M. G. Allen, M. R. Prausnitz, "Insertion of Microneedles Into Skin: Measurement and Prediction of Insertion Force and Needle Fracture Force", *J. Biomech.*, vol. 37(8), pp. 1155-1163, 2004.

[16] S. Nicoli, C. Padula, V. Aversa, B. Vietti, P.W. Wertz, A. Millet, F. Falson, R. P. Feynman, "Characterization of Rabbit Ear Skin as a Skin Model for in vitro Transdermal Permeation Experiments: Histology, Lipid Composition and Permeability", *Skin Pharmacol. Physi.*, vol. 21, pp. 218-226, 2008.

[17] I. P. Dick, R. C. Scott RC, "Pig ear skin as an in-vitro model for human skin permeability", J. Pharm. Pharmacol., vol. 44, pp. 640-645, 1992.

[18] N. Sekkat, Y. N. Kalia, R. H. Guy, "Biophysical study of porcine ear skin in vitro and its comparison to human skin in vivo", J. Pharm. Sci., vol. 91, pp. 2376-2381, 2002.